International Journal of Fracture **117:** 375–392, 2002.

Mechanism of effects of warm prestressing (WPS) on apparent toughness of notched steel specimens Part II: Calculations and analyses

J.H. CHEN[1], H.J. WANG[1], G.Z. WANG[1], Z.Q. DONG[1] and X. CHEN[2]
[1]*Gansu University of Technology, Lanzhou Gansu 730050, P.R. China;*
[2]*Wuhan Iron and Steel CO., Wuhan 430080, P. R. China; (e-Mail: zchen@gsut.edu.cn)*

Received 18 September 2001; accepted in revised form 26 August 2002

Abstract. Based on the experimental results of Part I of present work, this paper describes results of FEM calculations and analyses in details which identified that the effect of tensile-warm pre-stressing (WPS) on improvement of the apparent toughness of notched specimens results from three factors i.e. the residual compressive stress, macroscopic blunting of the original notch, and prestrain-deactivating cleavage initiation. The effects of three factors are separated and is effective for each at various extents of prestressing specified with a prestress-ratio, P_0/P_{gy}, defining the prestressing load P_0 as a fraction of general yield load P_{gy}. For values of prestress-ratio lower than 1.0, the residual compressive stress acts as the main factor. Between 1.0 to 1.5 of prestress-ratio values, in addition to the residual compressive stress the macroscopic blunting plays increasing role. The effect of the prestrain-deactivating cleavage initiation presents at the prestress-ratio $P_0/P_{gy} \geq 1.2$. In the case of compressive-warm prestressing, the apparent toughness is deteriorated due to the residual tensile stress. The effects of complex cycles of WPS, with various steps of loading and unloading different in signs, are determined mainly by the loading step just before the fracturing step.

Key words: Warm prestressing, fracture toughness, notched specimen, HSLA steel, Prestrain-deactivating.

1. Introduction

A great amount of evidence has been accumulated which demonstrates the beneficial effects of warm prestressing (WPS) on improving of the apparent fracture toughness of precracked and notched specimens. In a widely cited paper (Nichols et al., 1968), Nichols attributed the beneficial effects to three mechanisms:

(1) Work hardening to prevent yield on reloading
(2) Local yield on preload introducing beneficial local stresses
(3) Change of shape of the tip of defect (notch-blunting)

Harrison and Fearnehough (Harrison and Fearnehough, 1972) explained the benefit shown by specimens which were fractured without unloading (i.e., without residual compressive stress) from the prestress level by the generation of large plastic zone at the notch root which modified the stress pattern on testing at low temperature as compared with a virgin specimen. This argument is consistent with the item (1) of Nichols.

Recent investigations of Reed and Knott (Reed and Knott, 1989, 1996a, b) emphasized the role of the local residual stress based on the observation that stress-relief heat-treatments after prestressing remove nearly all the beneficial effects of WPS. Tensile prestress cycles give rise to residual compressive stress then the condition of fracture at low temperature cannot be reached until the effect of residual stress is eliminated. The effect of notch blunting is ignored

by listing the facts, that in blunt notch specimen the blunting of original notch is negligible and the beneficial effect of WPS remains even when ductile microcracks occur at the tip of notches.

But by quantitative investigation of the effects of WPS, Stoeckl et al. (2000) reveals that 'the WPS effect is well correlated with the crack blunting. The latter retards the stress intensification with increasing applied load'.

In reference of (Reed and Knott, 1989) Reed and Knott suggested a microcrack blunting mechanism that during the prestress operation the large inclusions experiencing high local stress due to dislocation pile up mechanism, will decohere and blunt out. Such a microcrack blunting mechanism would effectively prevent the larger inclusions from playing a role in subsequent initiation micro-mechanisms in lower shelf region fracture toughness test, and cleavage would initiate from smaller inclusions and the intrinsic toughness would be raised. This effect was named prestrain-deactivating cleavage initiation.

In a non-monotonic loading process the near-tip elastic-plastic fields are expected to be load-path dependent, such that in general it cannot be uniquely characterized by a J-integral alone. Chell et al. (1981) suggested a parameter J_e, which evaluates the force on all mobile dislocations enclosed by a contour, which separates the plastic and residual zones. The stress distribution at a crack tip subjected to a WPS cycle can be obtained by the superposition of the appropriate monotonic loading stress distributions evaluated by J_e. Curry (1983) further combined this model and the cleavage fracture criteria specified by RKR model (Ritchie et al., 1973) to predict the effects of WPS and strain aging.

Shum (1995) carried out comprehensive FEM calculations to quantitatively describe the path-dependent non-monotonic-loading near-tip crack-tip field. Besides the traditional explanation attributing the WPS effects to the residual compressive stress, the progressive loss of constraint was suggested as an alternative explanation for absence of crack initiation in monotonic unloading process.

From the review introduced above it is apparent that the mechanism of WPS effects is still an attractive subject. This paper describes the results of a comprehensive FEM calculation carried out for various regimes of Loading-unloading-cooling-fracturing (LUCF) cycles and a great variety of WPS operations with complex loading and unloading steps different in signs. Analyses are focusing on the roles played separately by the residual compressive stress, macro-blunting of original notch and the prestrain-deactivation of cleavage initiation by micro-blunting of conventional second phase particles in notched specimens.

2. Calculations

Based on the experimental results described in Part I of this paper, comprehensive FEM calculations were carried out with ABAQUS code to reveal the variations of distributions of normal stresses, plastic strains and stress triaxialities below the root of notches of specimens experiencing a great variety of LUCF cycles and cycles with complex loading and unloading steps different in signs.

Figure 1 shows the mesh arrangement in the region adjacent to the notch root. Eight elements are arranged around the notch root with a radius of 0.25 mm. 8-node biquadratic plane strain elements with reduced integration and hybrid elements (CPE8RH) are used for meshes experiencing heavy strain. 8-node biquadratic plane strain elements (CPE8) are used for remainders.

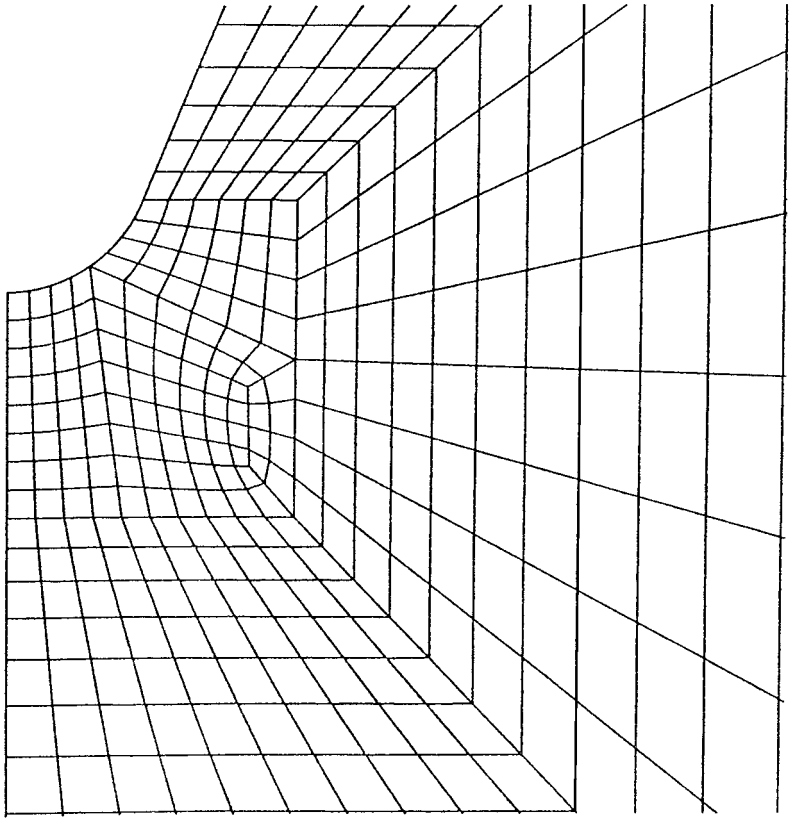

Figure 1. Arrangement of FEM mesh adjacent to the notch root

Because low cycle fatigue tests of HSLA steel WCF62 show the Bauchinger effect (Part I, Figure 4) with a sum of tensile and compressive yielding stress of about 1080 MPa and without isotropic hardening in non-monotonic stressing process, nonlinear kinematic hardening model is used in this work. By fitting the measured stress-strain curve parameters are calibrated and following expressions are used to represent constitutional relations at various temperatures. ???

$$\sigma_{\text{flow}} = 533 + 4000/7[1 - \exp(-7\varepsilon\text{p})] \quad \text{at } 20^{\circ}\text{C}$$

$$\sigma_{\text{flow}} = 964 + 1000/7[1 - \exp(-7\varepsilon\text{p})] \quad \text{at } -196^{\circ}\text{C}$$

Where ??? ε_{p} =íthe plastic strain, Young's modulus E=200000 MPa

Loading, unloading, cooling, and fracturing each takes a calculation step in LUCF process. Loading, the prestressing step is scaled by a prestress-ratio P_0/P_{gy} defining the prestressing load P_0 as a fraction of general yielding load P_{gy}.

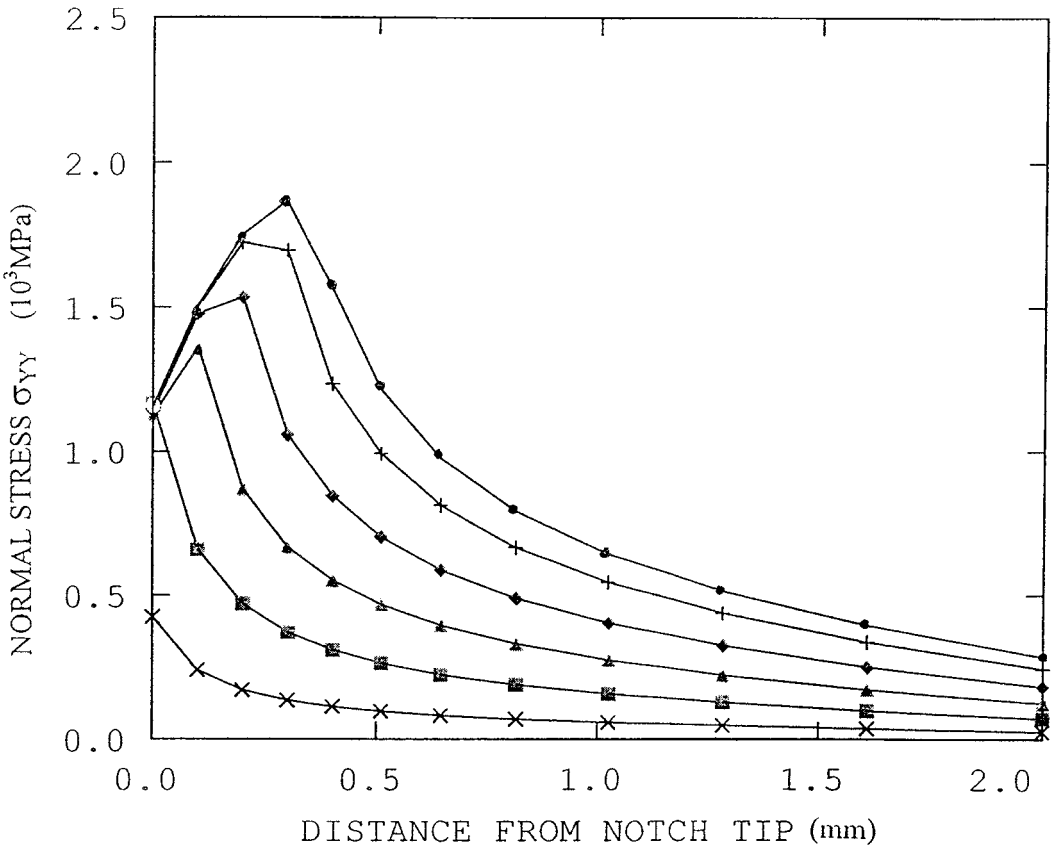

Figure 2. Normal stress distributions ahead of notch root developed during fracturing step at −196 °C × P=2.21KN; ■ P=6.10KN; ▲ P=10.53KN; ♦ P=14.95KN; + P=19.38KN; ●P=22.15KN

3. Results and analyses

3.1. Results of calculation for LUCF cycles with various prestress-ratios P_0/P_{gy}

3.1.1. *Tensile principal stresses ahead of notch roots*

Figures 2 and 3 show the distributions of the normal stress ahead of notch roots developed during the fracturing steps for specimens of directly Cooling-Fracturing (CF), and Loading-Unloading-Cooling-Fracturing cycle (LUCF) with prestress-ratio $P_0/P_{gy} = 1.0$, respectively.

From distribution curves of the normal stresses ahead of notch roots developed during the fracturing steps of specimens with various prestress-ratios (such as Figures 2 and 3 and X_f, the fracture initiation distances measured in Part I, the local fracture stresses σ_f were obtained (Chen et al., 1990) and the range of measured values are shown in Table 1 together with that of fracture loads P_f.

From Table 1 it is revealed that with increasing prestress-ratio P_0/P_{gy} the local fracture stress σ_f keeps almost in the same range around 1600 MPa, although the apparent toughness of notched specimens characterized by mean values of fracture load P_f apparently increase. It means that the effect of improving apparent toughness by WPS does not result from an enhancement of σ_f. Based on the criterion for cleavage of $\sigma_{yy} \geq \sigma_f$ it is reasonable to infer

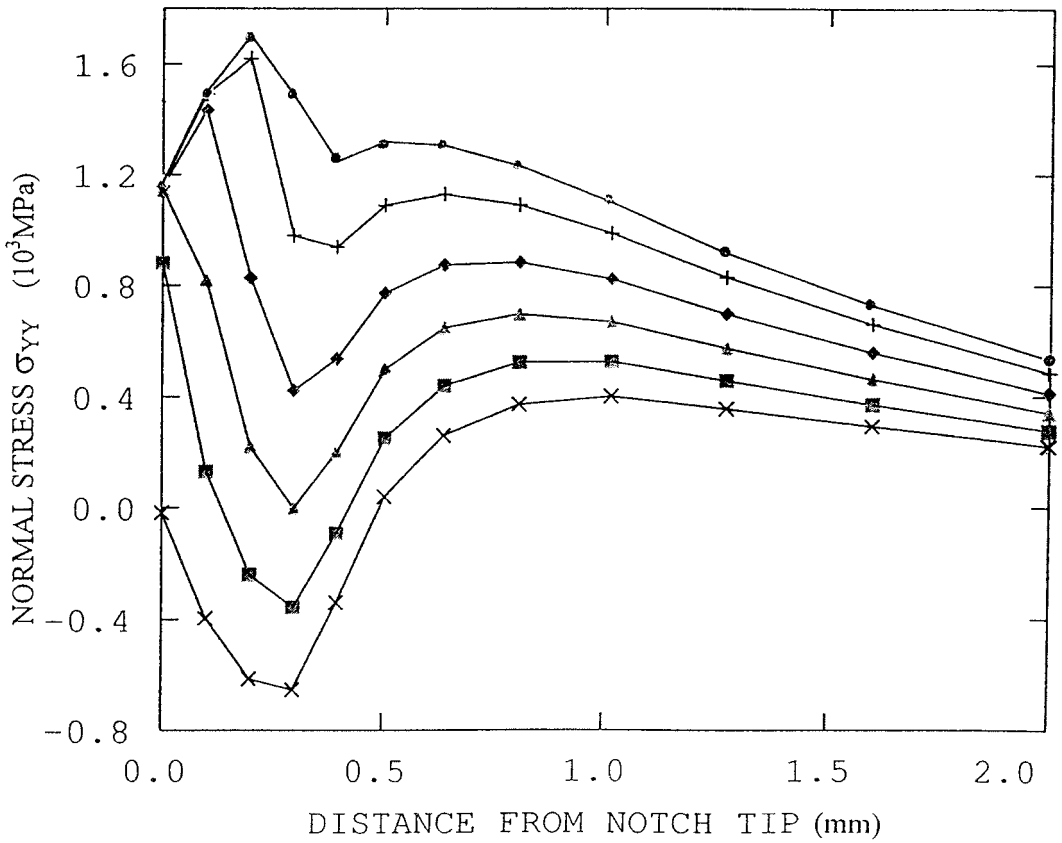

Figure 3. Normal stress distributions ahead of notch root developed during fracturing step at −196 °C of LUCF process with P_0/P_{gy} = 1.0× P=2.73KN; ■ P=7.52KN; ▲ P=12.99KN ♦ P=18.45KN; +P=23.92KNKg; ●P=27.34KN

that with increasing pre-stressing at room temperature, the load, necessary to intensify the tensile principal stress σ_{yy} to exceed the σ_f for fracturing at low temperature, increases. In other words at same applied load the tensile principal stress produced is lower for higher pre-stressed specimen. Table 2 shows the tensile principal stresses σ_{yy} reached at a distance of 200 μm from the notch root, (around this distance most of cleavage were initiated,) together

Table 1. Fracture loads and local fracture stresses measured in specimens with various prestress-ratio of LUCF

P_0/P_{gy}	P_f (KN)*	X_f (mμ)	σ_f (MPa)
0	16.66-22.15/19.14	129-210/135	1573-1630
0.5	16.95-19.11/18.20	88-150/120	1460-1603
0.8	20.34-26.46/22.51	105-590/226	1500-1668
1.0	21.56-27.34/23.77	70-263/190	1527-1629
1.2	19.60-29.11/24.58	90-420/236	1530-1670
1.5	35.28-41.65/39.03	178-258/231	1553-1696

*The denominators in column P_f present the mean values

Table 2. Tensile principal stress reached at a distance of 200 μm and peak values at applied load of 19.6KN at −196 °C

P_0/P_{gy}	0	0.5	0.8	1.0	1.2	1.5
σ_{yy} (MPa)	1723	1640	1550	1510	1520	1553
σ_{max} (MPa)	1730	1686	1550	1510	1520	1553

Table 3. Peak compressive stress and its location ahead of notch root after unloading from various prestress-ratio

P_0/P_{gy}	0	0.5	0.8	1.0	1.2	1.5
Peak Compressive stress (MPa)	0	−698	−825	−871	−746	−344
Distance from notch root(μm)	–	100	198	246	373	750

with their peak values σ_{max} at an applied load of 19.6KN at −196 °C. These values present the rates at which the tensile principal stresses σ_{yy} increase with increasing applied loads at the fracturing step.

From Table 2 it is apparent that with increasing the prestress-ratio P_0/P_{gy} up to 1.0 the tensile principal stress ahead of notches produced by same applied loads at same distance decreases remarkably. With further increasing prestress-ratio it increases slightly.

This phenomenon explains partly the effect of improvement of apparent toughness by WPS. Because at an applied load of 19.6KN, tensile principal stresses reach the value of σf (around 1600 MPa) for specimens with prestress-ratio $\leq$ 0.5, these specimens fractured at an applied load around 19.6KN. In specimens with prestress-ratio higher than 0.8 tensile principal stresses ahead of notches are insufficient to trigger cleavage at an applied load less than 19.6KN. The mechanism by which the tensile principal stress decreases with increasing prestress-ratio is discussed as follows:

3.1.2. *Residual compressive stress*

It is found that the trend of variation of tensile principal stress ahead of notch root with increasing prestress-ratio shown in Table 2 is consistent with that of residual compressive stress produced after unloading step of LUCF cycles. Figure 4 shows the distributions of residual compressive stresses after unloading step of LUCF cycle with various prestress-ratios. Table 3 shows the values of peak residual compressive stress and their location.

From Figure 4 and Table 3 it is revealed that with increasing prestress-ratio up to 1.0 the peak residual compressive stress increases and then decreases but the distance covered by compressive stress increases all along.

Compared with Table 2 it may be concluded that the residual compressive stresses which reduce the rates of intensification of tensile principal stresses ahead of notches, is the main factor improving the apparent toughness of notched specimens.

The decrease of residual compressive stress with increasing prestress-ratio from 1.0 to 1.5 results from the Bauschinger effect under heavy tensile pre-stress. Figure 5 compares the residual compressive stresses produced in the Unloading step of LUCF specimens with prestress-ratio of 1.0 and 1.5. With increasing the prestress-ratio up to 1.0 the residual com-

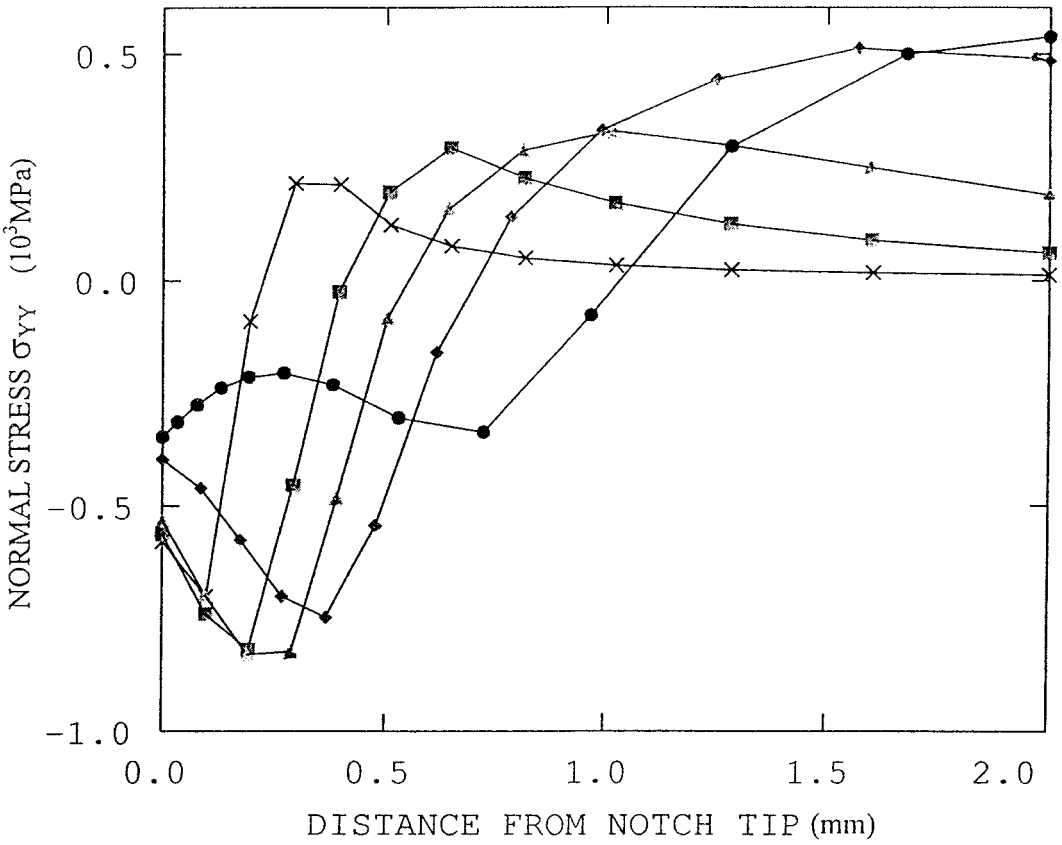

Figure 4. Distributions of residual compressive stress ahead of notch roots after unloading step ×$P_0/P_{gy} = 0.5$; ■ $P_0/P_{gy} = 0.8$; ▲ $P_0/P_{gy} = 1.0$; ♦ $P_0/P_{gy} = 1.2$; ● $P_0/P_{gy} = 1.5$

pressive stress increases due to the increasing compressive strain induced by the plastic strain produced in the prestressing step. Further increasing prestress-ratio up to 1.5 the flow stress developed at the notch root in prestressing step is high up to more than 1000 MPa. In this case under the effect of Bauschinger which limits the sum of tensile plus compressive yield stress equaling 1080 MPa, the compressive yield stress at the notch root presented in the unloading step is lower and the residual compressive stress developed from this lower yield stress is lower than that developed in specimens with prestress-ratio = 1.0.

By comparing Table 2 and Table 3 it will be inquired why a remarkable drop in values of residual compressive stress (from −871 to −344 MPa), presented in specimens with prestress-ratio higher than 1.0, results in only a bit increase of tensile principal stress (from 1510 to 1553 MPa in Table 2), if the residual compressive stress acts as the main factor decreasing the tensile principal stress. It is found that the blunting of notches plays increasing role in the event.

3.1.3. *Blunting of original notch*

Figure 6 shows the variations of open displacements of nodes located at the intersections of notch root with the blank side of specimens during LUCF cycles with prestress-ratio of 1.0 and 1.5.

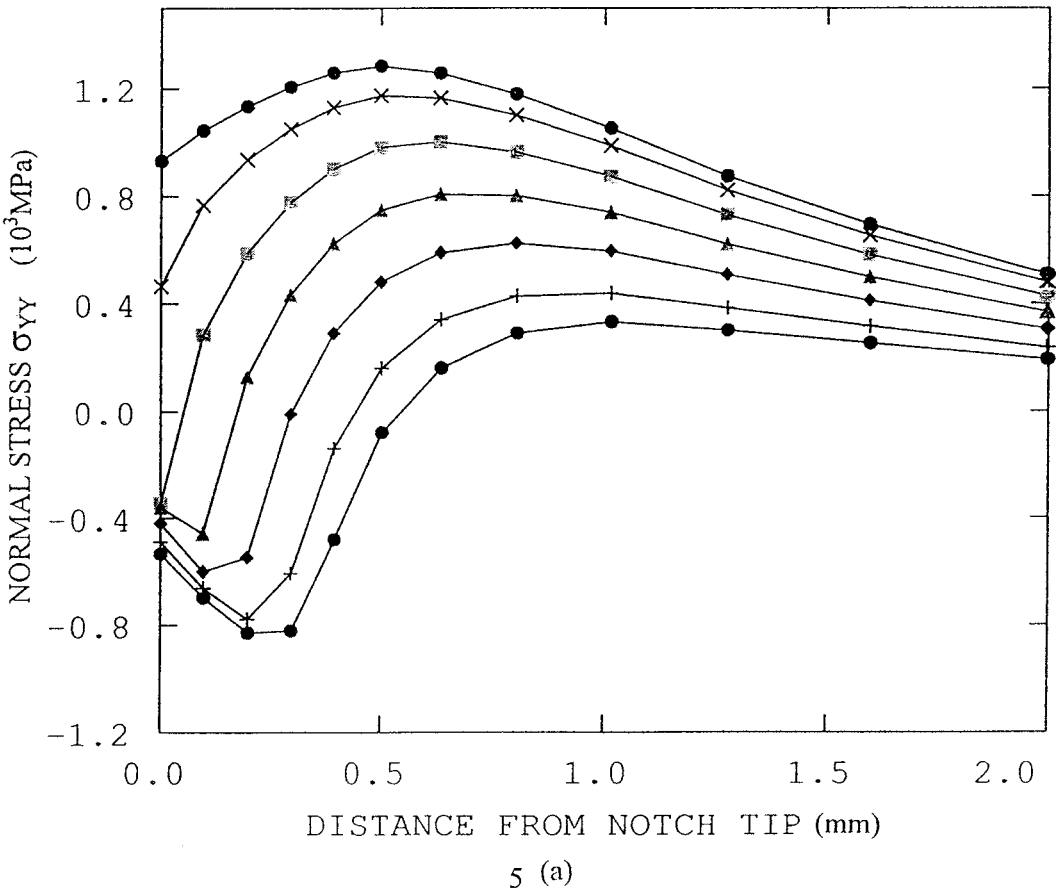

Figure 5. Distributions of residual compressive stresses produced during Unloading step of LUCF specimens with P_0/P_{gy} = 1.0(a): •P=24.65KN, ×P=22.19KN; ■P_0 = 17.95KN; ▲P=12.94KN; ♦P=7.94KN; +P=3.07KN; ●P=0 and P_0/P_{gy} =1.5(b): •P=36.75KN, ×P=33.08KN; ■P=26.65KN; ▲P=19.30KN; ♦P=11.95KN; +P=4.59KN; ●P=0

Figure 6 indicates that the opening displacement of the notch of specimen with prestress-ratio ≤ 1.0, after loading and unloading steps, is negligibly small (8.7 μm) compared to the original root radius (250 μm) but that of specimens with prestress-ratio of 1.5 is larger than the diameter of original notch root (307 μm vs. 250 μm). This trend of increase of notch opening displacement is consistent with experimental observations in Part I though the absolute values deviate in the P_0/P_{gy} range less than 1.0. Thus in specimens with prestress-ratio less than 1.0 the effect of notch blunting can be neglected but for specimens with prestress-ratio higher than 1.0 it is expected to be significant. For the former the decrease of tensile principal stress ahead of the notch can be mainly attributed to the residual compressive stress induced by prestressing and unloading steps. In specimens with prestress-ratio higher than 1.0 the effect of notch bunting plays increasing role by reducing the stress triaxiality developed during the fracturing step. This explains the lower increase of tensile principal stress than that expected from the decrease of residual compressive stress in specimens with $P_0/P_{gy} \geq 1.2$.

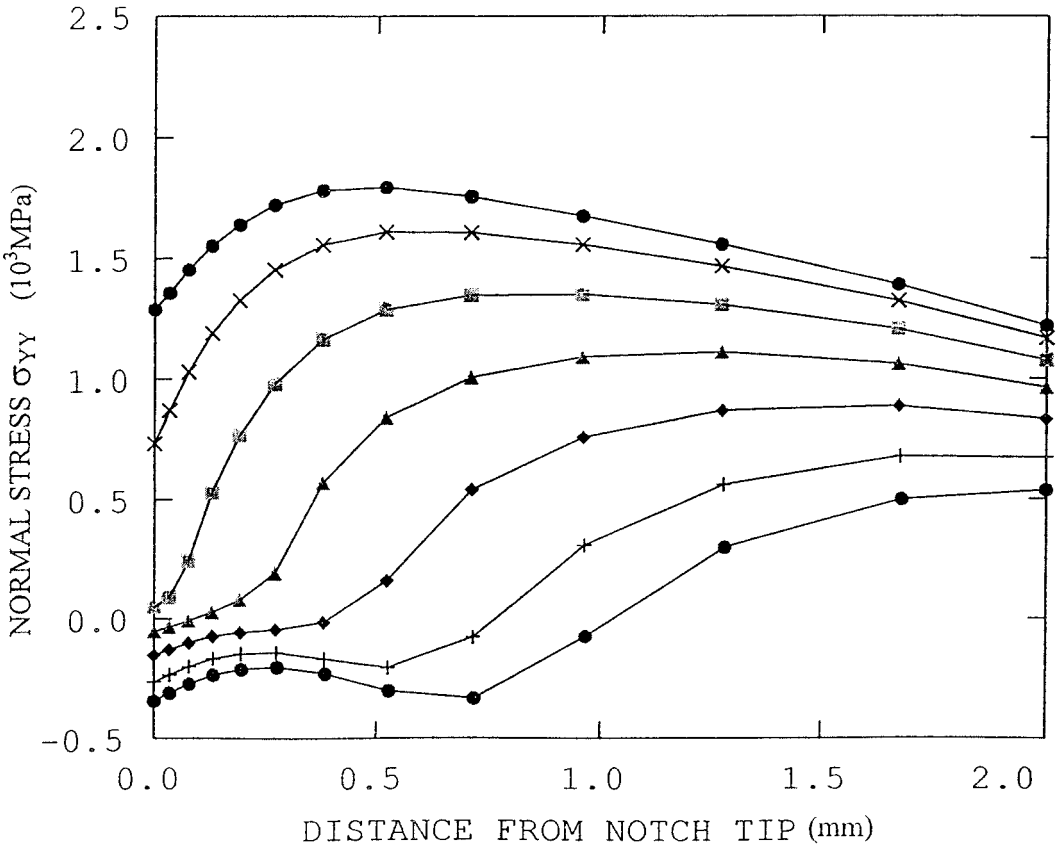

(b)

Figure 5. Continued.

Table 4. Stress triaxialities at a distance of 200 μm at applied load of 19.6KN

P_0/P_{gy}	0	1.0	1.2	1.5	FLUCF	FLULUCF
σ_m/σ_e	1.134	1.060	0.960	0.853	1.195	0.966

3.1.4. *Stress triaxiality σ_m/σ_e*

The stress triaxiality is defined as σ_m/σ_e, where $\sigma_m = 1/3(\sigma_{xx} + \sigma_{yy} + \sigma_{zz})$ is the mean or hydrostatic stress, ??? $\sigma_e = \sqrt{1}/2((\sigma_{xx} - \sigma_{yy})^2 + (\sigma_{yy} - \sigma_{zz})^2 + (\sigma_{zz} - \sigma_{xx})^2)$ is the equivalent stress. The tensile stresses ahead of the notch root are intensified to values much higher than the yield stress by the high stress triaxiality.

Table 4 shows the calculated values of stress triaxialities σ_m/σ_e at a distance of 200 μm ahead of notch roots of specimens with various prestress-ratio of LUCF, and FLUCF (reverse Loading-unloading-Cooling-Fracturing) and FLULUCF (reverse Loading-Unloading-Loading-Unloading) cycles at an applied load of 19.6KN.

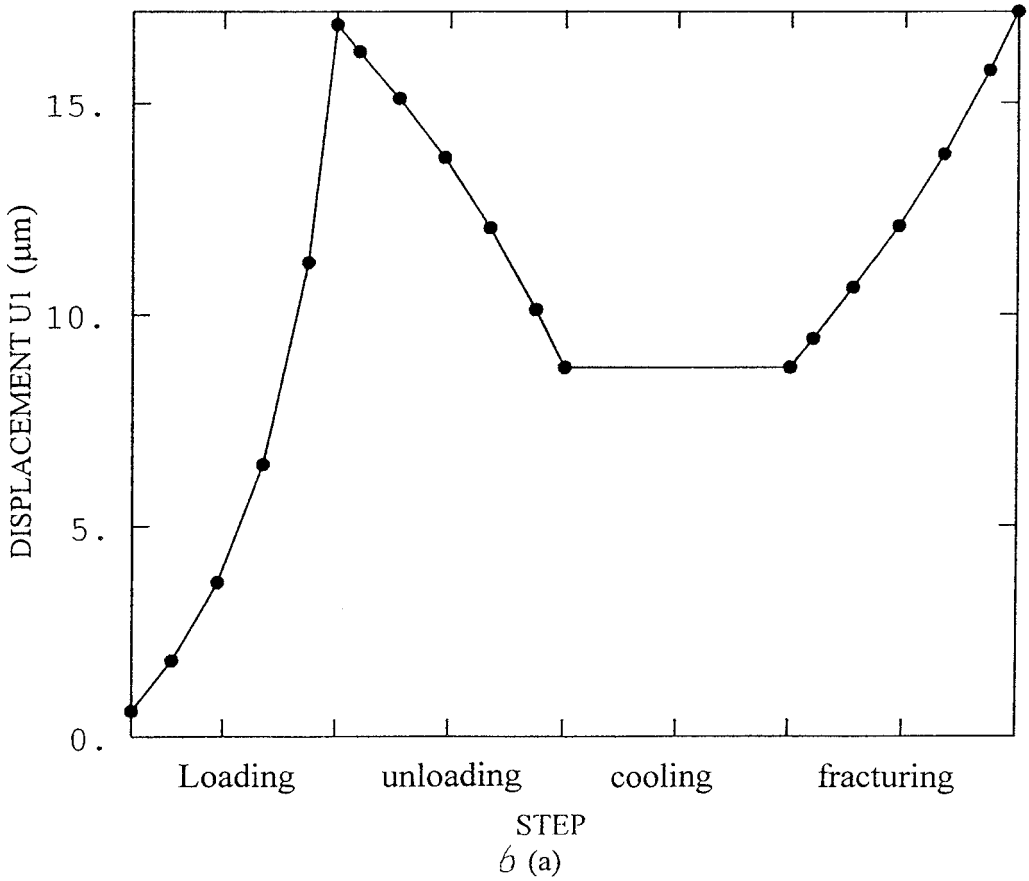

Figure 6. Opening displacements of notches in specimens with prestress-ratio of 1.0(a) and 1.5(b)

Table 4 shows appreciable reduce of stress triaxiality induced by notch blunting in specimens with $P_0/P_{gy} \geq 1.2$ which is considered to compensates the effect of drop of residual compressive stress (shown in Table 3) and keep the tensile principal stress at a lower level shown in Table 2. By analyzing the distribution curves of stress triaxialities ahead of notch roots in specimens with prestress-ratio ≤ 1.0, reduces of stress triaxialities compared to specimens CF without prestressing (shown in Table 4) can be attributed to the effect of residual compressive stress rather than to the notch blunting. Residual compressive stress not only directly decreases the increase rate of tensile principal stress σ_{yy} but also prohibits the intensification of triaxiality by reducing the lateral tensile stresses σ_{xx} and σ_{zz} i.e. by releasing the lateral constraint from the neighboring region where tensile stress is low due to the residual compressive stress. This fact can be envisaged by the curve showing the applied load of 13.0KN and 18.45KN in Figure 3. At notch root the tensile stresses reach the yield stress, but ahead of the notch due to the lower triaxiality the tensile stress cannot be intensified to high values.

In addition to the residual compressive stress the blunting of original notch, which has the tensile principal stress kept in a lower level in specimens with prestress-ratio higher than 1.0 (shown in Table 2) contributes to the improvement of apparent notch toughness. But by comparing Table 1 and Table 2 the further remarkable improvement of apparent toughness

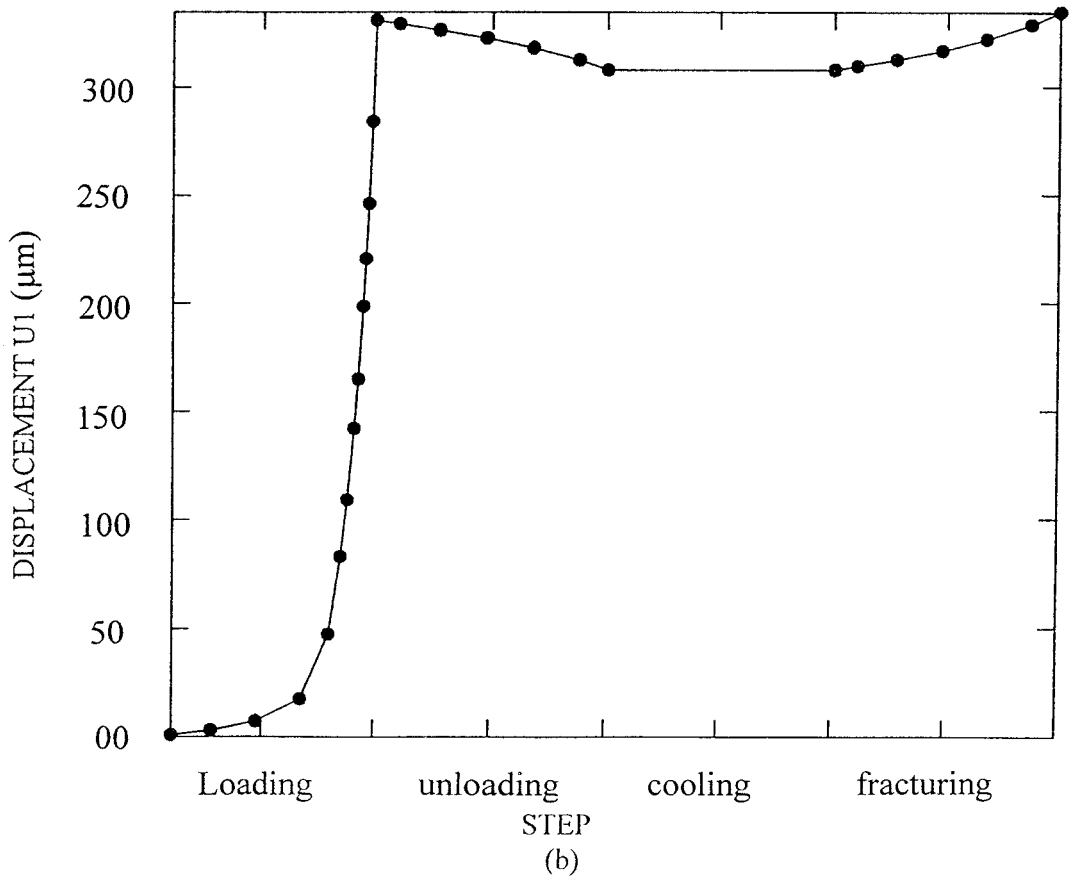

Figure 6. Continued.

Table 5. Critical plastic strain of specimens with various prestress-ratios

P_0/P_{gy}	0	0.5	0.8	1.0	1.2	1.5
$\varepsilon_{pc}(\%)$	1.0-2.0	1.0-1.5	1.5-1.7	1.1-1.9	1.7-3.0	2.1-3.4

by WPS with prestress-ratio$\geq$ 1.2 cannot be solely explained by the reduced tensile principal stress which contrarily increases a bit compared with those in specimens with prestress-ratio of 1.0.

This phenomenon can not been explained by the mechanism of cleavage with only a criterion of $\sigma_{yy} \geq \sigma_f$ and is analyzed as follows:

3.1.5. *Effect of the prestrain-deactivating cleavage initiation*

Table 5 shows the critical plastic strain ε_{pc}, the plastic strain at the cleavage initiation site accumulated during the last fracturing step of LUCF cycle.

From Table 5 it is revealed that for specimens with prestress-ratio ≤ 1.0 critical plastic strains for cleavage initiations drop in same range of 0.010-0.020. When the prestress-ratio reaches 1.2 the critical plastic strain increases appreciably. Accordingly the cleavage initiation sites move closer to the notch root compared with the location of the peak principal

Table 6. Distances from notch roots to points with various accumulated plastic strain ε_p

ε_p distance (μm)	0.005	0.01	0.02	0.05	0.10
P_0/P_{gy}					
0.5	274	142	28	–	–
0.8	555	309	150	–	–
1.0	801	436	240	68	–
1.2			476	276	142
1.5				904	658

stress. For explaining this phenomenon the distributions of plastic strain ε_p accumulated at the prestressing step are investigated and the results are shown in Table 6.

From Table 6 it is found that in specimens after prestressing with prestress-ratio ≥ 1.2, in the sensitive distance around 200 μm the plastic strain reaches 0.05 to 0.10. As indicated by Cox and Low (Cox and Low, 1974) in notched specimens of a commercial 18Ni maraging high strength steel when the true strain reaches 0.05 to 0.1 all of titanium-carbon-nitride second phase particles have voids associated with them. It means that at the true strain level of 0.05 to 0.1 voids nucleated at all of Ti(CN) particles. Refereed to this argument and by comparing Table 5 and Table 6 it is reasonable to infer that in specimens after prestressing with prestress-ratio ≥ 1.2 within a distance around 200 μm from notch root, all of conventional second phase particles will decohere and blunt out. Decohering of second phase particles and blunted cavities are observed in front of notch roots of specimens with $P_0/P_{gy} \geq 1.2$ in Part I. Such a microcrack blunting mechanism will effectively prevent these inclusions from playing a role in subsequent initiation micro-mechanisms in lower shelf region fracture toughness test. Therefore at the last fracturing step for nucleating cleavage the necessary plastic strain (0.02 to 0.03 in Table 5 for $P_0/P_{gy} \geq 1.2$) should be higher than the conventional one (0.01 to 0.02 in Table 5 for $P_0/P_{gy} \leq 1.0$). Thus higher load should be applied to create higher plastic strain although the tensile principal stress σ_{yy} has much more exceeded the local fracture stress σ_f. It means that for specimens with prestress-ratio higher than 1.2 the prestressing plays a role of prestrain-deactivating cleavage initiation and in addition to the effects of residual compressive stress and blunting of the notch root further remarkably improves the apparent toughness of material. In specimens with prestress-ratio less than 1.2 at the distance around 200 μm the plastic strain accumulated during prestressing step is less than 0.05. In this case some second phase particles eligible as cleavage nuclei remain and the critical plastic strain for initiating cleavage keeps in same level of 0.01 to 0.02 in specimens with P_0/P_{gy} from 0 to 1.0.

In summary, the main factors improving the apparent toughness by WPS in LUCF cycles can be concluded as the residual compressive stress, macroscopic blunting of the original notch, and prestrain-deactivating cleavage initiation which is effective for each at various extents of P_0/P_{gy}. For values of prestress-ratio lower than 1.0, the residual compressive stress acts as the main factor. Between 1.0 to 1.5 of prestress-ratio values the macroscopic blunting plays increasing role. The effect of the prestrain-deactivating cleavage initiation presents after the prestress-ratio reaches 1.2.

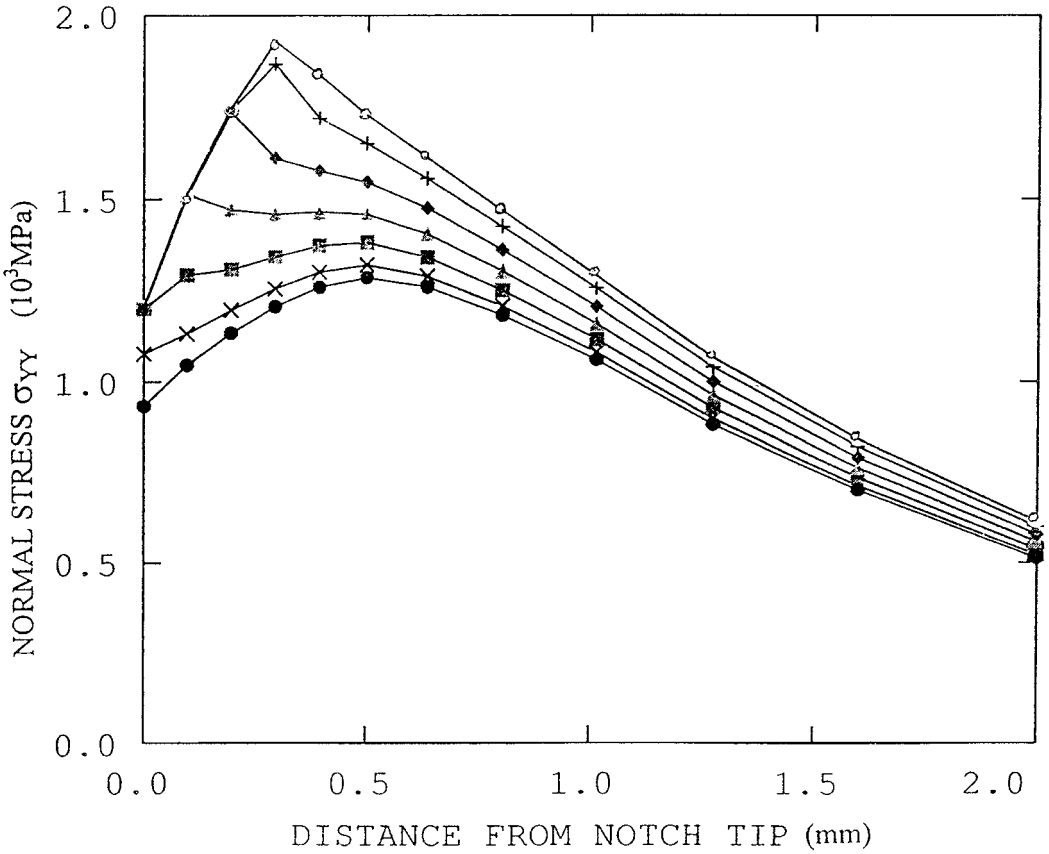

Figure 7. Distributions of tensile principal stress ahead of notch roots developed during the fracturing step of LCF cycle at −196 °C ●P=24.75KN, ×P=25.52KN; ■P=26.86KN; ▲P=28.39KN; ♦P=29.94KNKg; +P=32.11Kg; ○P=32.44KN

Because all of three factors are not algebraically additive in notched specimens the effects of WPS can not be obtained by superposition of the appropriate monotonic loading stress distributions evaluated by Je or applied loads as indicated by Chell (Chell et al., 1981) and Curry (Curry, 1983).

When the prestress-ratio approaches 1.8, there are microscopic cracks occurring at the notch root, the measured apparent toughness decreases again as shown by Figure 5 in Part I of this paper. It means the effect of microscopic cracks can not be ignored.

Calculation results for LCUF (Loading-Cooling-Unloading-Fracturing) cycle are similar to those for LUCF cycles. It is consistent with the experimental results that these two types of WPS cycles give rise almost the same improvement effects on the apparent notch toughness.

3.2. Results of calculation for LCF (Loading-Cooling-Fracturing) cycle

Figure 7 shows the tensile principal stress distribution in front of notch root developing during the fracturing step of LCF cycle at −196 °C from a prestressing load of 24.75KN applied at room temperature.

From Figure 7 and Xf, the distance of cleavage origin measured in Part I the local fracture stress σ_f could be obtained. As expected, σ_f has the measured values around 1550 MPa, in the same range of that measured in CF and LUCF cycles.

From calculation results for LCF cycle following ideas can be drawn:

1. The peak tensile principal stress σ_{max} reached at a preload of 24.75KN is 1279 MPa which is lower than the local fracture stress σ_f around 1600 MPa and is frozen to low temperature during the cooling step. Specimen cannot be fractured at the preload of 24.75KN during the cooling step.
2. Comparing Figure 2 and 7, same peak tensile principal stress of around 1600 MPa is reached at much lower applied load for CF cycle (16.66KN in Figure 2) than for LCF cycle (28.39KN in Figure 7). Therefore for reaching a maximum tensile principal stress of 1600 MPa equaling the σ_f, the necessary applied in LCF cycle is around 29.0KN yet it is only less than 16.66KN in CF cycle. These two figures are just the lower boundary values of fracture loads for LCF and CF cycles respectively. The improvement of apparent notch toughness by LCF cycle is mainly attributed to this effect.

By analyzing the variation of tensile principal stress at a fixed point it is found that during the cooling step a plastic condition reached at room temperature transfers to an elastic condition at -196 °C. The plastic constraint, the prerequisite for stress intensification, is lost. The stress intensification and thus the high tensile principal stress should be re-established along with the re-establishing of plastic zone at an applied load in excess of the preload though the increment is not very high. However a necessary plastic zone has been established at a much lower applied load in CF cycle. This is the physical mechanism of the positive effect of LCF cycle.

3. For specimens fractured at fracture load appreciably higher than 29.0KN (Part I Table V), the critical plastic strains at cleavage origin are measured to be close to 0.01 i.e. the lower limit for LUCF cycles. Thus the same critical plastic strain for nucleating a crack nucleus seems to be accumulated during the last fracturing step by an increment of applied load from the preload which makes the fracture load higher than the lower boundary fracture load (29.0KN) for $\sigma_{max} \geq \sigma_f$. This is a supplemental factor to further improve the apparent notch toughness in LCF cycle.

3.3. Results of calculating for various combinations of loading and unloading steps different in signs

3.3.1. *Local fracture stress*

From the calculated distributions of tensile principal stress ahead of notch roots developed during the fracturing steps for FLUCF (Reverse loading (in opposition direction)-Unloading-Cooling- Fracturing), LUfLUCF (Loading-Unloading-reverse Loading–Unloading-Cooling-Fracturing), and FLULUCF (Reverse loading-Unloading-Loading-Unloading-Cooling-Fracturing) cycles which are defined in Part I.

The local fracture stress σ_f is determined in each cycle. Table 7 shows the measured σ_f and the range of fracture loads P_f of specimens experiencing above WPS cycles and CF cycle for comparison.

From Table 7 it is found that the measured values of σ_f of specimens experiencing FLUCF, LUfLUCF, and FLULUCF processes drop in the same range of specimens experiencing LUCF processes with various prestress-ratios as shown in Table 1. It means that above WPS processes

Table 7. Fracture loads and local fracture stress of specimens with various regimes of WPS

Process	Fracture load P_f (KN)*	Local fracture stress σ_f (MPa)
FLUCF	9.31-10.68/10.18	1580
LUfLUCF	10.78-12.25/11.76	1500
FLULUCF	22.54-29.89/27.12	1500
CF	16.66-22.15/19.14	1573-1630

*The denominators in column P_f present the mean values

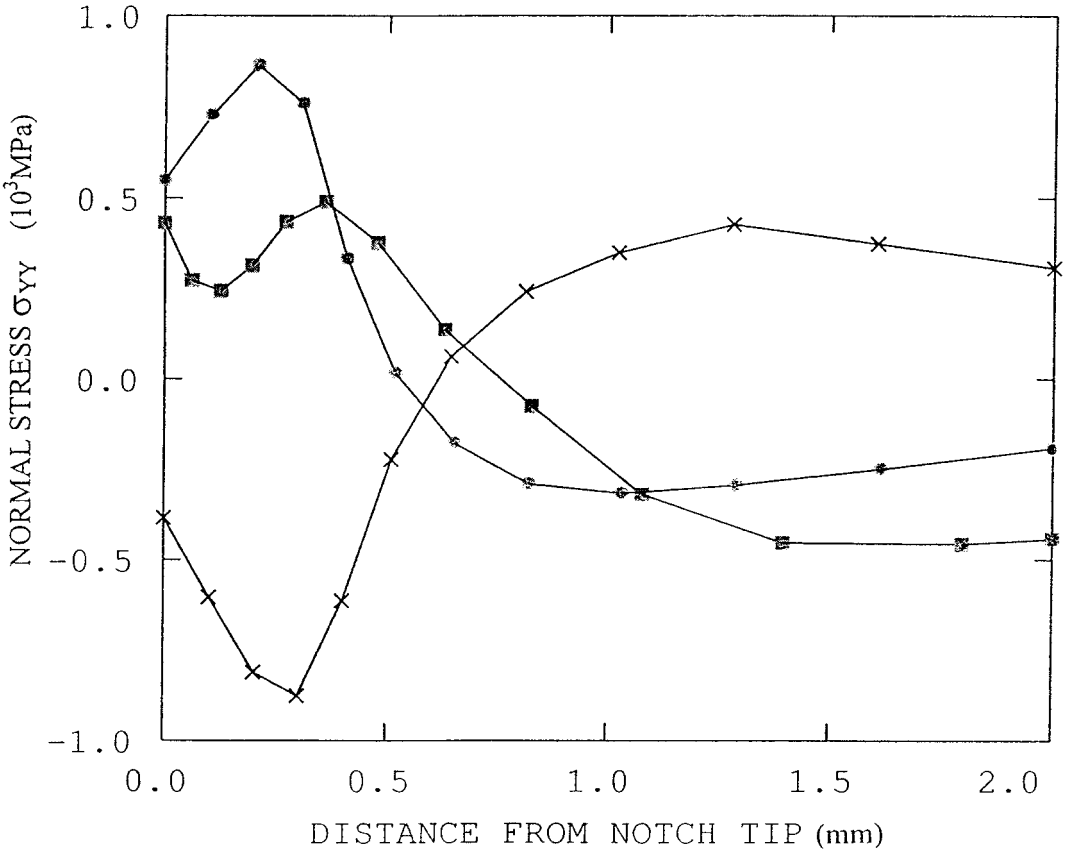

Figure 8. Residual stress distributions in specimens experiencing various WPS processes ×FLULUCF; ■LUfLUCF; ●FLUCF

put little effect on the real fracture toughness of materials. The variation of apparent toughness of specimens can be analyzed as follows:

3.3.2. *Factors affecting the apparent toughness presented in specimens with various loading and unloading steps different in signs*

Figure 8 shows the residual stress distributions in specimens experiencing various loading and unloading steps different in signs.

It is revealed that the apparent toughness of specimens varies in close relation with the variation of residual stress ahead of notch root. Apparent toughness of specimen experiencing FLULUCF cycle with residual compressive stress ahead of its notch root is higher than that of the directly fractured specimens CF without WPS. Oppositely the values of apparent toughness of LUfLUCF and FLUCF specimen with residual tensile stresses ahead of their notch roots are lower than that of specimens CF and the higher the residual tensile stress the lower the apparent toughness.

In specimen FLULUCF before the last fracturing step the notch opening is adjusted close to the original value, therefore the effect of notch blunting is excluded. The peak residual compressive stress just before the last fracturing step is -849 MPa and the tensile principal stress intensified at a distance of 200 μm by an applied load of 19.6KN is only 1530 MPa. These figures are close to those of specimen of LUCF with prestress-ratio of 1.0 and much lower than that in specimen CF without WPS shown in Table 2 and Table 3. Because the effect of notch blunting is excluded these results identify the effect of residual compressive stress on the improvement of apparent toughness. But the apparent toughness of FLULUCF specimen is appreciably higher than that of LUCF specimen with prestress-ratio of 1.0. It can be attributed again to the effect of the prestrain-deactivating cleavage initiation as in the cases of LUCF specimens with prestress-ratios ≥ 1.2. In specimen of FLULUCF the critical plastic strain ε_{pc} to trigger cleavage is up to 0.03, which is considered to be caused by heavily strained in first step of reverse-loading to 1.2 P_{gy} and in third step of reloading to 1.2 P_{gy}.

Due to the residual tensile stress in specimen FLUCF the tensile principal stress at 200 μm ahead of notch roots reaches 1700 MPa (Larger than the local fracture stress σ_f) at an applied load as low as 9.8KN at the last fracturing step which is much less than at an applied load of 19.6KN in specimen of CF. In addition to the residual tensile stress the higher stress triaxiality (shown in Table 4) caused by sharpening the notch root by reverse-loading step also intensifies the tensile principal stress and deteriorates the apparent toughness.

In specimens LUfLUCF two levels of reverse-Loading are carried out i.e. LUfLUCF and LUhfLUCF in Part I which really make the notch opening smaller and larger than the original one. In both cases the apparent toughness are similar and are lower than that in CF specimens as shown in Table 7. It means that the effect of deteriorating apparent toughness is not caused by sharpening the notch root by reverse-Loading and identifies the exclusive effect of residual tensile stress. The effect of the prestrain-deactivating cleavage initiation induced by the heavily pre-loading and reverse-loading cannot compensate the detrimental effect of residual tensile stress.

In summary, experiments and calculations for specimens with complex loading and unloading steps different in signs which separate the effects of residual stress from notch blunting identify the effects of three main factors i.e. the residual stress, macroscopic deformation of the original notch, and prestrain-deactivating cleavage initiation on improvement of apparent toughness and indicate the deteriorative effect of residual tensile stress.

The effects of WPS of LUCF process indicated above are different from those presented in a precracked specimen (Chen et al., 2001). In the latter case because the precrack is much sharper than a notch, the crack blunting by WPS is a fundamental factor for improving the apparent toughness by reducing the stress triaxiality and plastic strain produced in the fracture step. In precracked specimens the residual compressive stress plays only a secondary role instead of the main role as in the notched specimens.

It should be notified that in this work the residual compressive stress presents benefit effects in steel showing Bauchinger effect without isotropic hardening in non-monotonic stressing

process. As indicated in Results 3.1.2, the Bauschinger effect limits the sum of tensile plus compressive yield stress to around 1080 MPa, heavy compressive stress developed in the unloading step limits the tensile yield stress in the step of fracturing. In steel without Bauchinger effect due to the work hardening effect affecting in every step the yielding stress will be much higher than the original value. In regions where a tensile plastic strain is re-established the tensile principal stress, intensified from the hardened high yield stress, is much higher than that in specimen of steel showing Bauschinger effect without isotropic hardening. Therefore in specimens where the tensile plastic strain can be re-established at lower applied load such as at a precrack tip, the benefit effect induced by the residual compressive stress may be offset by the effect of work hardening (Chen et al., 2002).

4. Conclusion

From experiments, calculations, and analyses carried out for notched specimens of WCF62 HSLA steel experiencing various warm pre-stressing (WPS) cycles, following conclusions can be drawn:

(1) Specimens experiencing Load-Unload-Cool-Fracture (LUCF) cycles with various prestress-ratios show that the effect of tensile (normal) warm prestressing (WPS) on improvement of the apparent toughness of notched specimens results from three factors i.e. the residual compressive stress, macroscopic blunting of the original notch, and prestrain-deactivating cleavage initiation. For values of prestress-ratio lower than 1.0, the residual compressive stress acts as the main factor. Between 1.0 to 1.5 of prestress-ratio values addition to the residual compressive stress the macroscopic blunting plays a increasing role. The effect of the prestrain-deactivating cleavage initiation presents after the prestress-ratio reaches 1.2.

(2) Specimens experiencing various regimes of WPS process with complex loading and unloading steps different in signs which separate the effect of residual stress from that of notch root blunting and produce both residual compressive stress and residual tensile stress identify further effects of the three factors revealed by LUCF process. The residual compressive stress benefits the apparent toughness yet the residual tensile stress remarkably deteriorates it.

(3) At the last fracturing step, the re-establishment of a tensile strained area with sufficient plastic strain at a distance for nucleating a crack nucleus is a necessary condition for triggering cleavage i.e. $\varepsilon_{\mathrm{p}} \geq \varepsilon_{\mathrm{pc}}$. The criterion of $\sigma_{\mathrm{yy}} \geq \sigma_{\mathrm{f}}$ is a sufficient condition for cleavage. The three factors mentioned in (1) and (2) play their roles through putting effect on the driving force. While the plastic deformation experienced during WPS cycles may change the critical value $\varepsilon_{\mathrm{pc}}$.

Acknowledgement

This work was financially supported by the National Natural Science Foundation of China (No. 59871015) and the Key Research and Development Program for Outstanding Groups of Gansu University of Technology.

References

Chell, G.G., Haigh, J.R. and Vitek, V. (1981) A theory of warm prestressing: experimental validation and the implications for elastic plastic failure criteria. *International Journal of Fracture* **17**, 61–81.

Chen, J.H., Zhu, L. and Ma, H. (1990) On the scattering of the local fracture stress σ_f. *Acta Metall. Mater.* **38**, 2527–2535.

Chen, J.H., Wang, V.B., Wang, G.Z. and Chen, X. (2001), Mechanism of Effects of Warm Prestressing on Apparent Toughness of Precracked Specimens of HSLA Steels. *Engng. Fract. Mech.* **68**, 1669–1686.

Chen, J.H., Pippan, R., Hebesberger, T. and Kolednik, O. (2002) The fracture behavior of intermetallic TiAl alloys with and without warm prestressing, *Inter. J. Fract.* **113**, 327–343.

Cox, T.B. and Low JR., J.R. (1974) An investigation of the plastic fracture of AISI 4340 and 18 nickel–200 grade maraging steel. *Metall. Trans.* **15**, 1457–1470.

Curry, D.A. (1983) A model for predicting the influence of warm pre-stressing and strain ageing on the cleavage fracture toughness of ferritic steels. *International Journal of Fracture* **22**, 145–159.

Harrison, T.C. and Fearnehough, G.D. (1972) The influence of warm prestressing on the brittle fracture structure containing sharp defects. *J. of Basic Engineering* june, 373–376.

Nichols, R.W., Kienzler, R. and Nagel, G. (1968) The use of overstressing techniques to reduce the risk of subsenquent brittle fracture. Part I: *British Welding J.* **15**, 21–42 and 75–84.

Reed, P.A.S. and Knott, J.F. (1989) Warm prestressing effects in notched bars of a MnNiMo steel weld-metal. *Adv. Res. Fract. Proc. Of ICF7* Vol. 4. Pergamon, New York, pp. 2583–2593.

Reed, P.A.S. and Knot, J.F. (1996a) Investigation of the role of residual stressing in the warm prestress (WPS) effect, Part I- experimental. *Fatigue Fract. Engng Mater. Struct.* **19**, 485–500.

Reed, P.A.S. and Knot, J.F. (1996b) Investigation of the role of residual stressing in the warm prestress (WPS) effect, Part II-analysis. *Fatigue Fract. Engng Mater. Struct.* **19**, 501–513.

Ritchie, R.O., Knott, J.F. and Rice, J.R. (1973) On the relationship between critical tensile stress and fracture toughness in mild steel. *J. Mech. Phys. Solids* **21**, 395–410.

Shum, D.K.M. (1995) Interpretation of warm prestress-induced fracture toughness based on crack-tip constraint. *Fracture Mechanics: 25th volume, ASTM STP 1220* Ed. F. Erdogan, 686–704.

Stoeckl, H., Boeschen, R., Schmitt, W., Varfolomeyev, I. and Chen, J.H. (2000) Quantification of the warm prestressing effect in a shape welded 10 MnMoNi5-5 material. *Engng. Fract. Mech.* **67**, 119–137